analytical chemistry

Subscriber access provided by UNIV OF CAMBRIDGE

Article

Simultaneous Fluorescence Imaging Reveals NMDA Receptor Dependent Zn/H Flux in the Brains of Mice with Depression

Xin Wang, Xiaoyi Bai, Di Su, Yandi Zhang, Ping Li, Shuyi Lu, Yulin Gong, Wen Zhang, and Bo Tang

Anal. Chem., **Just Accepted Manuscript** • DOI: 10.1021/acs.analchem.9b05771 • Publication Date (Web): 10 Feb 2020

Downloaded from pubs.acs.org on February 11, 2020

Just Accepted

"Just Accepted" manuscripts have been peer-reviewed and accepted for publication. They are posted online prior to technical editing, formatting for publication and author proofing. The American Chemical Society provides "Just Accepted" as a service to the research community to expedite the dissemination of scientific material as soon as possible after acceptance. "Just Accepted" manuscripts appear in full in PDF format accompanied by an HTML abstract. "Just Accepted" manuscripts have been fully peer reviewed, but should not be considered the official version of record. They are citable by the Digital Object Identifier (DOI®). "Just Accepted" is an optional service offered to authors. Therefore, the "Just Accepted" Web site may not include all articles that will be published in the journal. After a manuscript is technically edited and formatted, it will be removed from the "Just Accepted" Web site and published as an ASAP article. Note that technical editing may introduce minor changes to the manuscript text and/or graphics which could affect content, and all legal disclaimers and ethical guidelines that apply to the journal pertain. ACS cannot be held responsible for errors or consequences arising from the use of information contained in these "Just Accepted" manuscripts.

is published by the American Chemical Society. 1155 Sixteenth Street N.W., Washington, DC 20036

Published by American Chemical Society. Copyright © American Chemical Society. However, no copyright claim is made to original U.S. Government works, or works produced by employees of any Commonwealth realm Crown government in the course of their duties.

Simultaneous Fluorescence Imaging Reveals NMDA Receptor Dependent Zn^{2+}/H^{+} Flux in the Brains of Mice with Depression

Xin Wang‡, Xiaoyi Bai‡, Di Su, Yandi Zhang, Ping Li*, Shuyi Lu, Yulin Gong, Wen Zhang and Bo Tang*

College of Chemistry, Chemical Engineering and Materials Science, Key Laboratory of Molecular and Nano Probes, Ministry of Education, Collaborative Innovation Center of Functionalized Probes for Chemical Imaging in Universities of Shandong, Institutes of Biomedical Sciences, Shandong Normal University, Jinan 250014, People's Republic of China.

ABSTRACT: Depression is immensely attributed to the over-activation of N-methyl-D-aspartic acid (NMDA) receptor in the brains. As regulatory binding partners of NMDA receptor, both Zn^{2+} and H^{+} are intimately interrelated to NMDA receptor's activity. Therefore, exploring synergistic changes on the levels of Zn^{2+} and H^{+} in brains will promote the knowledge and treatment of depression. However, the lack of efficient, appropriate imaging tools limits simultaneously tracking Zn^{2+} and H^{+} in living mouse brains. Thus, a well-designed dual-color fluorescent probe (DNP) was fabricated for the simultaneous monitoring of Zn^{2+} and H^{+} in the brains of mice with depression. Encountering Zn^{2+}, the probe evoked bright blue fluorescence at 460 nm. Meanwhile, the red fluorescence at 680 nm was decreased with H^{+} addition. With blue/red dual fluorescence signal of DNP, we observed the synchronous increased Zn^{2+} and H^{+} in PC12 cells under oxidative stress. Notably, *in vivo* imaging for the first time revealed the simultaneous reduction of Zn^{2+} and pH in brains of mice with depression-like behaviors. Further results implied that NMDA receptor might be responsible for the coinstantaneous fluctuation of Zn^{2+} and H^{+} during depression. Altogether, this work is conducive to the knowledge of neural signal transduction mechanisms, advancing our understanding of the pathogenesis in depression.

Depression possesses high morbidity and mortality, substantially contributing to the global burden of disease and disability.[1] However, current diagnoses and treatments for depression are inadequate, mainly due to the rudimentary understanding about the pathogenesis of depression.[2,3] N-methyl-D-aspartic acid (NMDA) receptor, a subtype of the ionic glutamate receptor, is an essential ion channel protein that maintains normal nervous functions, such as the development of neurons and synaptic plasticity.[4,5] Previous studies suggest that over-activation of NMDA receptor plays a critical role in the physiology and pathology of depression.[6-8] Furthermore, several antidepressants, such as dizocilpine, are conferred with the antidepression effect as antagonists of NMDA receptor.[9,10]

Zinc is the second abundant d-zone metal in the brain, which is widely distributed in the hippocampus, regulating learning and long-term memory.[11,12] The abnormal homeostasis of Zn^{2+} in nervous system is correlated with a variety of cerebral diseases, such as Alzheimer's disease and depression.[13,14] Furthermore, Zn^{2+} could be released from glutamatergic vesicles to regulate the activity of NMDA receptor, which is always accompanied by neuronal activity or depolarization.[15] In the meantime, H^{+} can modulate the neurons' function by regulating various voltage-gated and ligand-gated ion channels, such as NMDA receptor.[16-19] Altogether, as regulatory binding partners of NMDA receptor, Zn^{2+} and H^{+} are both intimately interrelated to the activity of NMDA receptor.[20-22] Therefore, exploring synergistic changes on the levels of Zn^{2+} and H^{+} in brains will promote the knowledge and treatment of depression. However, the lack of efficient, appropriate imaging tools limits simultaneously tracking Zn^{2+} and H^{+} in living mouse brains.

With the merit of high spatial-temporal resolution, real-time visualization and non-destructive, fluorescence imaging technique has becoming a robust method for investigating biological events in living cells and *in vivo*.[23-25] Recently, many fluorescent probes have been developed for the detection of Zn^{2+} or H^{+} in living cells and small animals.[26-29] However, the coinstantaneous fluctuation of Zn^{2+} and H^{+} in brains are still undefined due to the particularly complicated construction of the brain and the lack of appropriate probe. Therefore, specific probes capable of simultaneous monitoring Zn^{2+} and H^{+} with high spatial-temporal resolution in brains of mice are in a great demand.

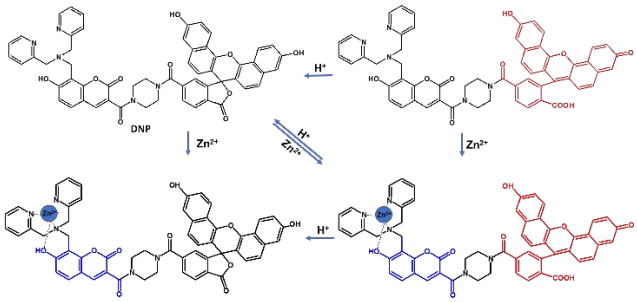

Scheme 1. The Structure and Luminescence Mechanism of DNP.

Thus, we fabricated an original fluorescent probe (DNP) for the simultaneous *in situ* detection of Zn^{2+} and H^{+}. As shown in Scheme 1, DNP is composed of a Zn^{2+}-specific

group and a H^+-sensitive moiety that enable synchronously dynamic responses to Zn^{2+} and H^+. Notably, dual-color (blue/red) fluorescence imaging for Zn^{2+} and H^+ can be simultaneously achieved at different excitation, 390 nm or 610 nm, severally. Using DNP, we visualized the fluctuation of Zn^{2+} and H^+ under the over-activation of glutamate receptor NMDA in PC12 cells. Furthermore, changes of Zn^{2+} and H^+ in the brains of mice with depression were successfully mapped for the first time.

EXPERIMENTAL SECTION

Synthesis of the Probe. Compounds 1, 2 and 3 were synthesized as previously reported in references.[30,31]

Compound DNP: The compound 2 (0.416 g, 1.0 mmol) and compound 3 (0.476 g, 1.0 mmol) were added to 1-Hydroxybenzotriazole (0.203 g, 1.5 mmol), 1-(3-Dimethylaminopropyl)-3-ethylcarbodiimide hydrochloride (0.288 g, 1.5 mmol) and 2 mL DMF, 8 mL CH_2Cl_2. Then, the mixture was stirred for 10 min and then added piperazine (0.010 g, 1.2 mmol). Next, the mixture was stirred overnight at room temperature. The crude product was purified by TLC using CH_2Cl_2/CH_3OH (10:1) as the eluent to give DNP (0.28 g, 30 % yield). ^{1}H NMR (400 MHz, DMSO-d_6) 8.52(d, J=4.0 Hz, 2H), 8.10(d, J=4.0 Hz, 1H), 7.97(s, 1H), 7.95(d, J=1.2 Hz, 2H), 7.74(d, J=1.6 Hz, 1H), 7.71(d, J=4.0 Hz, 2H), 7.69(s, 2H), 7.52(d, J=0.8 Hz, 2H), 7.50(t, J=0.8 Hz, 2H) 7.48(d, J=0.8 Hz, 2H), 7.42(s, 1H), 7.40(d, J=0.8 Hz, 2H), 7.37(t, J=0.8 Hz, 2H), 7.36(d, J=0.8 Hz, 1H), 6.88(d, J=3.6 Hz, 1H), 5.27(t, J=4.4 Hz, 2H), 4.74(d, J=15.2 Hz, 1H), 3.95(s, 4H), 3.46(t, J=6.0 Hz, 4H), 3.42(s, 2H), 3.40(t, J=5.2 Hz, 4H). ^{13}C NMR (101 MHz, DMSO-d_6) 172.51, 168.99, 162.88, 162.73, 158.39, 157.92, 157.75, 157.66, 156.36, 155.60, 155.05, 154.33, 151.10, 150.24, 149.45, 148.81, 148.77, 146.66, 144.40, 144.28, 143.27, 137.61, 137.26, 136.53, 135.53, 130.80, 129.94, 128.28, 127.50, 126.68, 124.82, 124.28, 123.67, 123.45, 123.14, 122.99, 119.80, 119.53, 119.48, 117.81, 114.44, 113.77, 110.11,109.94, 109.59, 47.53, 46.10, 45.79, 41.39, 36.19, 31.19, 21.65, 21.47. HRMS (ESI), m/z calcd for $C_{56}H_{41}N_5O_{10}$ $[M+H]^+$ 944.2966, found 944.2926.

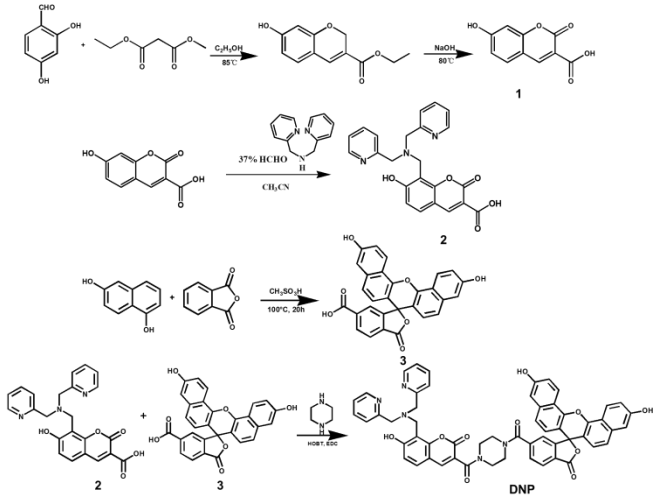

Scheme 2. Synthesis of DNP.

Confocal Imaging Experiments. One day before imaging, the cells were detached and replanted onto glass-bottomed dishes. After an incubation with the probe for 20 min, the cell culture media were removed and cells were washed with 1.0 mL PBS for three times. Fluorescence images of DNP (Zn^{2+}) were obtained with an excitation wavelength of 405 nm and blue channel was 420-500 nm. Fluorescence images of DiBAC were obtained with an excitation wavelength of 488 nm and green channel was 500-530 nm. Fluorescence images of DNP (H^+) were obtained at an excitation wavelength of 561 nm and red channel emission window was 630-730 nm. For data analysis, the average fluorescence intensity per image under each experimental condition was obtained by selecting regions of interest. Each experiment was repeated at least three separate times with identical results.

Intracellular pH Calibration. The PC12 cells were incubated with high K^+ buffer (30 mM NaCl, 120 mM KCl, 1 mM $CaCl_2$, 0.5 mM $MgSO_4$,1 mM NaH_2PO_4, 5 mM glucose, 20 mM HEPES and 20 mM NaOAc) at various pH values (6.5-8.0) in the presence of 10.0 μM of nigericin. After 30 min, DNP was added to cells and incubated for 20 min at 37 °C. The fluorescence images were captured, and the pH calibration curve was constructed with confocal microscope.

Mouse Models of Depression. We constructed C57 mice with depression by treatment with corticosterone (CORT), according to the references.[45-47]. After 3 weeks, sucrose preference test, forced swimming test, and tail suspension test were performed before imaging. Lighter weight and longer despair time in forced swimming test are considered as an index of depression. Only the mice with obvious reduction in preference for sucrose or significant increase in immobility were considered as the successful established depression model, which were allowed to imaging.

RESULTS AND DISCUSSION

Preparation and Optical Properties of DNP. We synthesized and characterized a new fluorescent probe for Zn^{2+} and H^+, designated DNP (6'-(4-(8-((bis(pyridin-2-ylmethyl)amino)methyl)-7-hydroxy-2-oxo-2H-chromene-3-carbonyl)piperazine-1-carbonyl)-3,11-dihydroxy-3'H-spiro[dibenzo[c,h]xanthene-7,1'-isobenzofuran]-3'-one) (Scheme 2). DNP consists a coumarin covalently linked DPA (2,2'-dipicolylamine) (λ_{ex} = 390 nm, λ_{em} = 460 nm) function as the Zn^{2+} indicator and a naphthalene fluorescein (λ_{ex} = 610 nm, λ_{em} = 680 nm) as the H^+ reporter. DPA quenches the

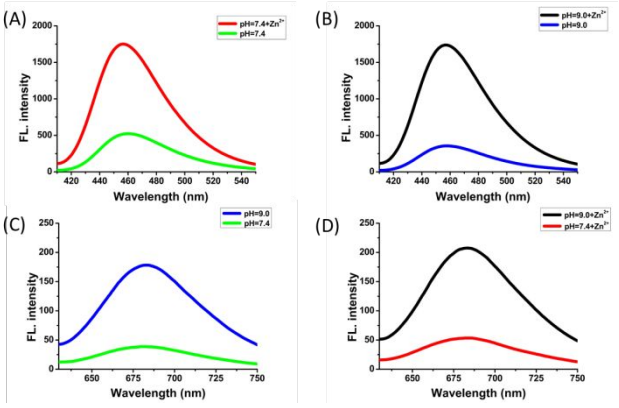

Figure 1. The different emission spectra for DNP (10 μM) before (green) and after (red) the addition of Zn^{2+} (10 μM) at pH = 7.4 and with the pH increased to 9.0 before (blue) and after (black) add Zn^{2+} (10 μM). (A, B) Fluorescence

spectral at 390 nm excitation. (C, D) Fluorescence spectral at 610 nm excitation.

fluorescence of coumarin through photoinduced electron transfer (PET). Encountering Zn^{2+}, PET would be blocked, causing bright blue fluorescence at 460 nm. Meanwhile, with H^+ addition, the red fluorescence at 680 nm is decreased due to the naphthofluorescein group in the probe transform to closed spirolactone structure from the open quinone form.

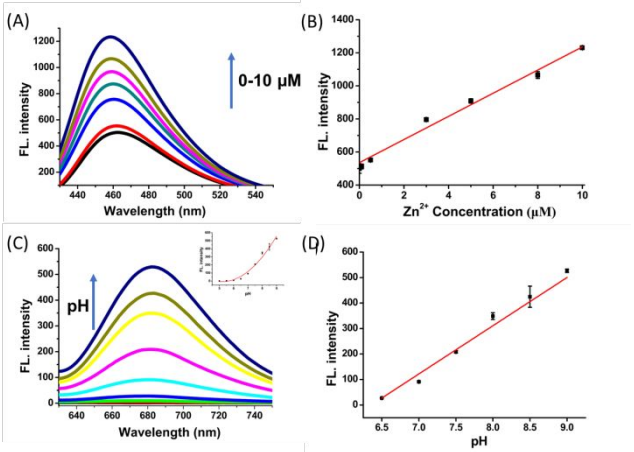

Figure 2. Fluorescent properties of the DNP for Zn^{2+} and pH detection. (A) Fluorescence spectra of 10 μM DNP after the addition of various concentrations of Zn^{2+} (0-10 μM). (B) Linear relationship of fluorescence intensity with Zn^{2+}. All of the data were acquired in 0.1 M Tris, pH 7.4, with λ_{ex} / λ_{em} at 390/460nm. (C) Fluorescence spectral changes of DNP (10 μM) with various pH values from 5.0 to 9.0. Insert: Fluorescence intensity vs. pH with λ_{ex} / λ_{em} at 610/680nm. (D) Linear relationship of fluorescence intensity with pH (6.5-9.0).

For evaluating the optical properties of DNP, we first tested its absorption spectra (Figure S1). DNP exhibited two absorption bands at approximately 390 nm (coumarin fraction) and 580 nm (naphthalene fluorescein fraction). After the addition of 10 μM Zn^{2+} at pH = 7.4, the absorption peak at 390 nm was enhanced. When the pH increased from 7.4 to 9.0, the absorption peak at 580 nm red-shifted to 610 nm. Then, we investigated the fluorescence responses of DNP to Zn^{2+} and pH, respectively. As exhibited in Figure 1A, upon excitation at 390 nm, DNP displayed dim fluorescence at 460 nm under simulated physiological conditions (0.1 M Tris buffer, pH = 7.4). Following the addition of 10 μM Zn^{2+}, the intensity of DNP at 460 nm clearly increased (3.5-fold), and the fluorescence quantum yield raised from 32 % to 52 %. Similarly, when the pH altered from 7.4 to 9.0, the fluorescence intensity of DNP at 680 nm under 610 nm excitation significantly enhanced (4.0-fold) (Figure 1C), the fluorescence quantum yield enlarged from 2 % to 7 % (Figure S2).[32] Besides, Figure 1 and Figure S3 demonstrate that the responses of DNP to Zn^{2+} and pH are not interferential to each other. Consistent with our design strategy, the probe is exquisite for the simultaneous detection of Zn^{2+} and H^+.

Based on those results, we examined the Zn^{2+}/H^+ concentration-dependent fluorescence intensities of DNP. As the concentration of Zn^{2+} elevated from 0 μM to 10 μM, the fluorescence intensity at 460 nm gradually enhanced followed by the linear equation F = 70.03 [Zn^{2+}] (μM) + 535.46 with the linear correlation coefficient of 0.991 (Figure 2A, B). Accordingly, the detection limit for Zn^{2+} was 0.32 μM, the complexation ratio was 1:1 (Figure S4), and the complexation constant was 3.94 μM. As the pH changed from 6.5 to 9, the fluorescence intensity at 680 nm stepwise increased by the linear equation F = 189.26[pH]–1203.00 with the linear correlation coefficient of 0.981. (Figure 2C, D).[33,34] These data verify that DNP can synchronously indicate Zn^{2+} and pH *via* dual-color, distinguishable fluorescence signals.

To explore the selectivity of DNP for Zn^{2+}/H^+, we examined the fluorescence responses in the presence of various biologically competed species. As exhibited in Figure S5A, the blue fluorescence of DNP displayed highly selectivity to Zn^{2+} without the interference of other metal ions, reactive oxygen species (ROS), and reactive nitrogen species (RNS), illustrating the DPA-based probe is highly specificity to Zn^{2+}. Moreover, the fluorescence response of DNP to Zn^{2+} was pH-insensitive (Figure S6). As depicted in Figure S5B and S5C, DNP exhibited nearly no change in fluorescence at 680 nm in the presence of metal ions, ROS, and RNS under various pH conditions, suggesting that DNP possesses the high selectivity for H^+. Furthermore, DNP presented other advantages, including excellent photostability (Figure S7), low cytotoxicity under 237 μM (Figure S8). Taken together, DNP can potentially act as a powerful fluorescence probe for the simultaneous indicating of Zn^{2+} and pH in the biological systems.

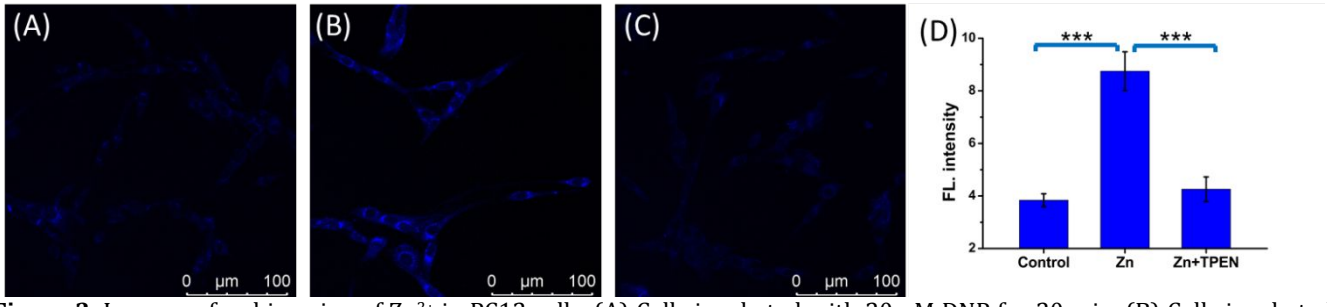

Figure 3. Laser confocal imaging of Zn^{2+} in PC12 cells. (A) Cells incubated with 20 μM DNP for 20 min. (B) Cells incubated with $ZnSO_4$ (50 μM) for 10 min and then with 20 μM DNP for 20 min. (C) Cells incubated with $ZnSO_4$ (50 μM) for 10 min, with TPEN (50 μM) for 10 min and then with 20 μM DNP for 20 min. (D) The fluorescence intensities of (A) – (C). λ_{ex} = 405 nm, collected 420-500 nm. The data are shown as the mean ± SD, n = 3, ***p <0.001.

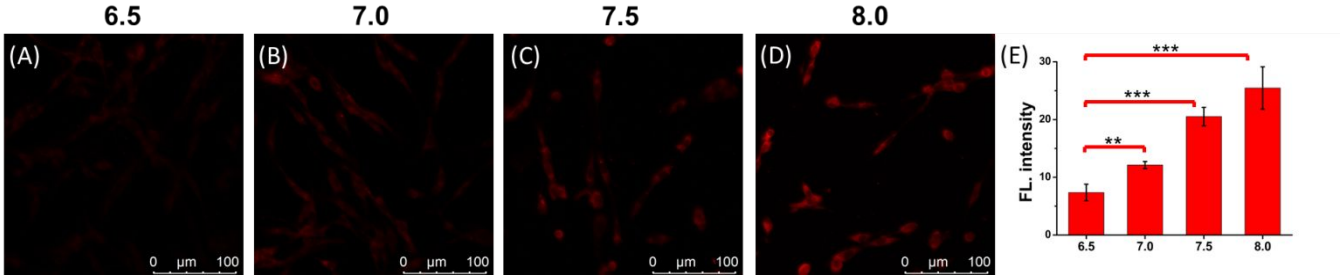

Figure 4. Fluorescent confocal microscopy images of DNP (20 μM) in PC12 cells at pH 6.5–8.0. (E) The fluorescence intensities of (A) – (D). λ_{ex} = 561 nm, collected 630-730 nm. The data are shown as the mean ± SD, n = 3, **p <0.01, ***p <0.001.

Fluorescence Imaging of Exogenous $Zn^{2+}$and H^+ in Living Cells with DNP. For verifying the performance of DNP in cells, we tracked Zn^{2+} and H^+ in PC12 cells under different conditions. We first visualized the exogenous Zn^{2+} and pH changes in the living PC12 cells. The blue fluorescence signal represented the fluctuation of Zn^{2+} concentration, and the red fluorescence signal indicated the H^+ levels. Compared with the control group, blue fluorescence in PC12 cells treated with Zn^{2+} (50 μM) significantly enhanced (about 2.2-fold). To prove that fluorescence changes indeed resulted from the variation in Zn^{2+}, the membrane-permeable metal ion chelator N,N,N',N'-tetrakis(2-pyridylmethyl)ethylenediamine (TPEN, 50 μM) were added to PC12 cells,[35] and the blue fluorescence obviously decreased, implying the selectivity of DNP to Zn^{2+} (Figure 3). Next, we treated cells with high K^+ concentration buffer with different pH and the ionophore ingericin to change H^+ level in cells.[36] Figure 4 showed that the red fluorescence within PC12 cells elevated accompanying with the pH (6.5–8.0) increased. The above imaging results testify that DNP is able to synergistically reflect the transient changes in Zn^{2+} and pH in living cells.

Simultaneous Imaging of Endogenous Zn^{2+}/H^+ in Living Cells with DNP. Next, we investigated the changes of endogenous Zn^{2+} and H^+ in PC12 cells by utilizing DNP. Previous researches have mentioned that high concentration of glutamate could induce oxidative stress in the nervous system,[37-39] which will cause the released of $Zn^{2+}$and H^+.[27,40,41] To explore the flux of Zn^{2+} and H^+ under oxidative stress, we treated PC12 cells with 10 mM glutamate to simulate the oxidative stress. Compared with the control cells, those cells pre-incubated with glutamate distinctly evoked bright blue fluorescence (1.6-fold) and paler red fluorescence, manifesting that the levels of Zn^{2+} and H^+ were both rising. To further prove that the brighter blue fluorescence was exactly caused by the boost of Zn^{2+}, we then used metal ion chelating agent TPEN to treated cells. As expected, the blue fluorescence intensity was significantly decreased, while the red fluorescence remained essentially stable (Figure 5). These data provide strong evidence that the Zn^{2+} and H^+ levels both elevated upon the oxidative stress. Besides, similar results were observed in PC12 cells stimulated by phorbol 12-myristate 13-acetate (PMA),[42] another oxidative stress trigger by activating PKC (protein kinase C) (Figure S9). Altogether, those data highlight the fact that DNP could simultaneously monitor endogenous Zn^{2+}/H^+ in living cells.

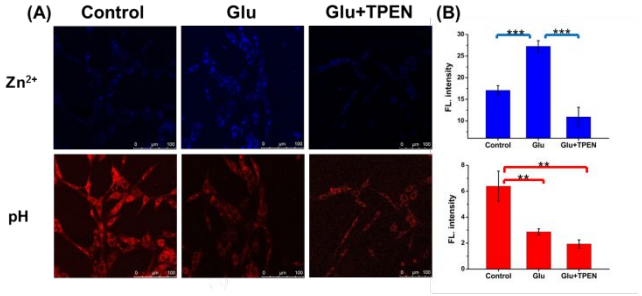

Figure 5. Laser confocal imaging in PC12 cells. (A) Control: PC12 cells incubated with 20 μM DNP for 20 min. Glu: PC12 cells incubated with 20 μM DNP for an additional 20 min after preincubation with 10 mM glutamate for 12 h. Glu+TPEN: PC12 cells incubated with 10 mM glutamate for 12 h, with TPEN (50 μM) for 10 min and then with 20 μM DNP for 20 min. (B) The data output from (A). Blue: λ_{ex} = 405 nm, collected 420-500 nm. Red: λ_{ex} = 561 nm, collected 630-730 nm. The values are the mean ± SD for n = 3, **p <0.01, ***p <0.001.

Imaging of Zn^{2+} and pH in Brains of Mice with Depression. Inspired by the successful application of DNP in the intracellular imaging, we evaluated the suitability of DNP in synchronously monitoring Zn^{2+} and H^+ fluctuations in brains of mice with depression. We constructed C57 mice with depression by treatment with corticosterone (CORT), according to the references .[43-47] Depression-like behaviour tests, such as Sucrose preference, tail suspension and forced swimming were performed to evaluate the success of the models (Figure S10).[48,49] After surgical exposure of the brains, the probe (100 μM) was directly added to the brain, and then those mice with depression-like behaviours were imaged. The *in vivo* imaging found that the Zn^{2+}-sensitive fluorescence signal and pH-response fluorescence signal both deceased in brains of mice with depression-like behaviors (Figure 6).[50,51] Therefore, these results provide strong evidence for simultaneous reduction in Zn^{2+} and pH in brains of mice with depression-like behaviours.

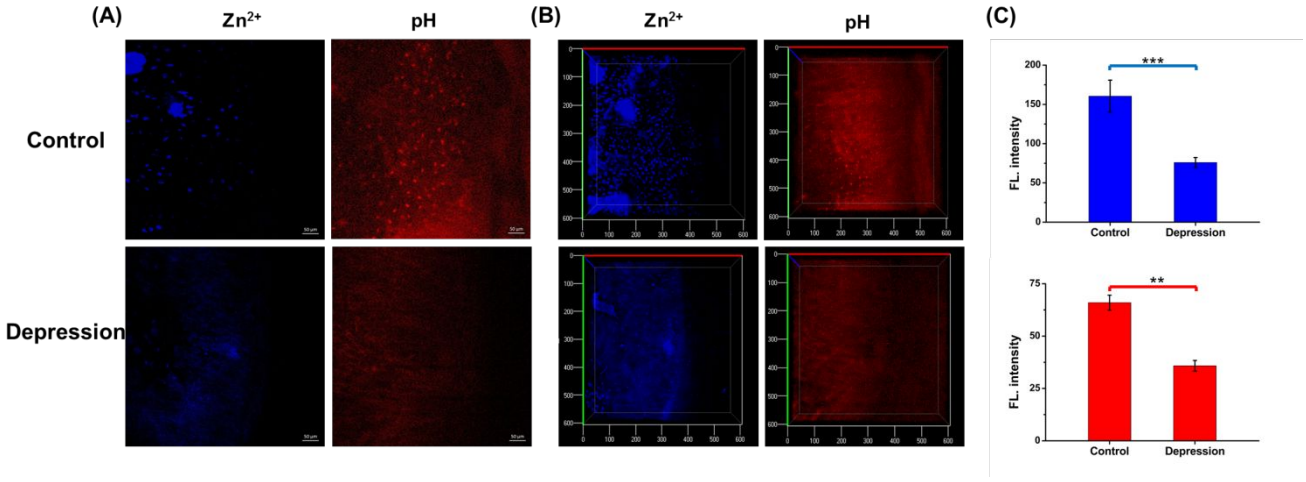

Figure 6. *In situ* two-photon imaging in brains of mice. (A) Imaging at 50 μm in the mouse brain. (B) 3D images with (A). (C) Relative fluorescence intensities of mice in (A). The 3D images were generated from a stack of cross sections (xy sections, 400 μm) with an axial (z) increment of 2 μm. Mice are representative images from repeated experiments (n = 3). Blue: λ_{ex} = 800 nm, collected 410-560 nm. Red: λ_{ex} = 633 nm collected 650-750 nm. The values are the mean ± SD for n = 3, **p <0.01, ***p <0.001.

Imaging of Zn^{2+} and H^+ in PC12 Cells under Over-activation of NMDA Receptor. Next, we initially investigated why Zn^{2+} and H^+ fluctuated during depression. Several studies have shown that over-activation of NMDA receptor plays critical role in the physiology and pathology of depression. As regulatory binding partners of NMDA receptor, there are close relationship between Zn^{2+}/H^+ and activity of NMDA receptor. As a Ca^{2+} channel, the NMDA receptors would increase the concentration of Ca^{2+} in cells when over-activated. Excess Ca^{2+} could over-activate the nitric oxide synthetase (a Ca^{2+}-dependent enzyme) and cause the generation of ROS, leading to the oxidative stress.[52,53] Then, the redox-sensitive Zn^{2+}-binding proteins such as metallothioneins would release Zn^{2+} under the oxidative stress.[54,55] Many studies have indicated that ROS could also inhibit the Na^+/H^+ exchanger (NHE) and acidify the neurons by increasing H^+.[41] Therefore, we further investigated if the NMDA receptor could mediate the levels of Zn^{2+} and H^+ in living cells. The commercial fluorescent probe DiBAC (λ_{ex} = 490 nm, λ_{em} = 505 nm, green fluorescence) for membrane depolarization was chosen as the indicator to monitor the activity of the NMDA receptor.[56] NMDA, the specific agonist of the NMDA receptor, was used to activate NMDA receptor. Utilizing DNP, the markedly increased blue fluorescence and the decreased red fluorescence was observed in those NMDA treated cells, manifesting the level of Zn^{2+} and H^+ rose. Meanwhile, those cells evoked obviously green fluorescence, proving the over-activation of NMDA receptor induced by NMDA.

To further prove that the changes of Zn^{2+} and H^+ are correlates with the activity of NMDA receptor, we incubated cells with NMDA receptor specific antagonist MK801.[57] Compared to NMDA treated cells, the weaker blue fluorescence and brighter red fluorescence were observed, demonstrating the decrease in the concentrations of Zn^{2+} and H^+ under the inhibition of NMDA receptor (Figure 7). Moreover, glutamate, the physiological agonist of the NMDA receptor, were also used to treat PC12 cells to activate NMDA receptor. Not surprise, similar imaging results were obtained, further implying that the over-activation of NMDA receptor could induce the elevated Zn^{2+} and H^+ (Figure S11). Overall, we drawn a conclusion that the activation of NMDA receptor caused the increase in levels of Zn^{2+} and H^+. Based on the current work, we speculated that the released of Zn^{2+} induced by the over-activation of NMDA receptors might bind to other proteins or flow away during depression. These results provide primary evidence for explaining the synchronous changes of Zn^{2+} and H^+ *in vivo*, which inspired us to focus on where Zn^{2+} going *in vivo* during depression in the future. Altogether, we provide a powerful imaging tool for simultaneous analysis of Zn^{2+} and H^+ *in vivo*.

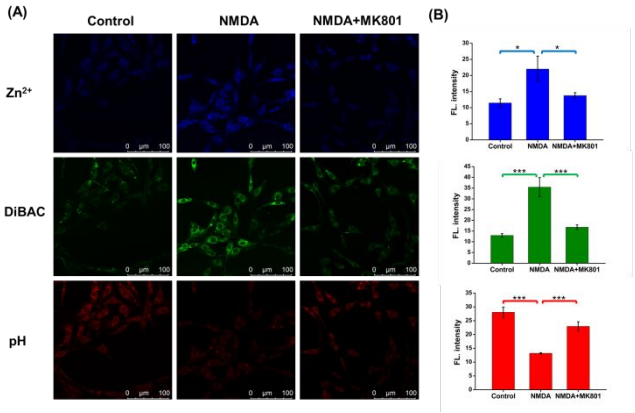

Figure 7. Laser confocal imaging in PC12 cells. (A) Control: PC12 cells incubated with 20 μM DNP for 20 min and then with 10 μM DiBAC for 15 min. NMDA: PC12 cells incubated with 20 μM DNP for 20 min and then with 10 μM DiBAC for 15 min after preincubation with 2.5 mM NMDA for 12 h. NMDA+MK801: PC12 cells incubated with 20 μM DNP for 20 min and then with 10 μM DiBAC for 15 min after preincubation with 2.5 mM NMDA and MK801 for 12 h. (B) The data output from (A). Cell images are representative images from repeated experiments (n = 3). Blue: λ_{ex} = 405 nm, collected 420-500 nm. Green: λ_{ex} = 488 nm, collected 500-530 nm. Red: λ_{ex} = 561 nm, collected 630-730 nm. The values are the mean ± SD for n = 3, *p <0.05, ***p <0.001.

CONCLUSION

In summary, we developed a robust fluorescent probe DNP for simultaneously monitoring Zn^{2+} and H^+ in mouse brains. Utilizing DNP, we mapped the increased Zn^{2+} and H^+ in PC12 cells under the oxidative stress. Of note, *in vivo* imaging for the first time revealed the simultaneous reduction of Zn^{2+} and pH in brains of mice with depression-like behaviors. Further results implied that the NMDA receptor might be responsible for the coinstantaneous fluctuation of Zn^{2+} and H^+ during depression. Altogether, this work provides strong and direct evidence for disclosing the relationships between Zn^{2+}, H^+ and depression, advancing our understanding of the pathogenesis during depression.

ASSOCIATED CONTENT

Supporting Information

The Supporting Information is available free of charge on the ACS Publications website.

Additional experimental data, including synthesis, characterization, photophysical properties, cytotoxicity, and experimental details.

AUTHOR INFORMATION

Corresponding Author

*E-mail: lip@sdnu.edu.cn
*E-mail: tangb@sdnu.edu.cn
ORCID
Bo Tang: 0000-0002-8712-7025

Author Contributions

‡These authors contributed equally.

ACKNOWLEDGMENT

This work was supported by the National Natural Science Foundation of China (21675105, 21535004, 91753111, 21927811), Key Research and Development Program of Shandong Province (2018YFJH0502), National Major Scientific and Technological Special Project for "Significant New Drugs Development" (2017ZX09301030004), and Natural Science Foundation of Shandong Province of China (ZR2017ZC0225).

REFERENCES

(1) Kessler, R. C.; Berglund, P.; Demler, O.; Jin, R.; Merikangas, K. R.; Walters, E. E. *Arch. Gen. Psychiatry* **2005**, 62, 768-768.

(2) Nestler, E. J.; Barrot, M.; DiLeone, R. J.; Eisch, A. J.; Gold, S. J.; Monteggia, L. M. *Neuron* **2002**, 34, 13-25.

(3) Krishnan, V.; Nestler, E. J. *Nature* **2008**, 455, 894-902.

(4) Carroll, R. C.; Zukin, R. S. *Trends Neurosci.* **2002**, 25, 571-577.

(5) Lau, C. G.; Zukin, R. S. *Nat. Rev. Neurosci.* **2007**, 8, 413-426.

(6) McCarthy, D. J.; Alexander, R.; Smith, M. A.; Pathak, S.; Kanes, S.; Lee, C.-M.; Sanacora, G. *Med. Hypotheses* **2012**, 78, 675-681.

(7) Valentine, G. W.; Sanacora, G. *Biochem. Pharmacol.* **2009**, 78, 431-439.

(8) Papp, M.; Moryl, E. *Eur. J. pharmacol.* **1994**, 263, 1-7.

(9) Skolnick, P.; Layer, R. T.; Popik, P.; Nowak, G.; Paul, I. A.; Trullas, R. *Pharmacopsychiatry* **1996**, 29, 23-26.

(10) Yang, Y.; Cui, Y.; Sang, K.; Dong, Y.; Ni, Z.; Ma, S.; Hu, H. *Nature* **2018**, 554, 317-322.

(11) Tamano, H.; Takiguchi, M.; Shimaya, R.; Adlard, P. A.; Bush, A. I.; Takeda, A. *Biochem. Biophs. Res. Commun.* **2019**, 514, 888-892.

(12) Sindreu, C.; Palmiter, R. D.; Storm, D. R. *Proc. Natl. Acad. Sci. U. S. A.* **2011**, 108, 3366-3370.

(13) Takeda, A.; Tamano, H. *Front. Aging Neurosci.* **2014**, 6, 26-32.

(14) Dou, M.; Gong, A.; Liang, H.; Wang, Q.; Wu, Y.; Ma, A.; Han, L. *Neurosci. Lett.* **2018**, 683, 196-201.

(15) Frederickson, C. J.; Koh, J. Y.; Bush, A. I. *Nat. Rev. Neurosci.* **2005**, 6, 449-462.

(16) Traynelis, S. F.; Cull-Candy, S. G. *J. Physiol.* **1991**, 433, 727-763.

(17) Yao, H.; Haddad, G. G. *Cell Calcium* **2004**, 36, 247-255.

(18) Waldmann, R.; Lazdunski, M. *Curr. Opin. Neurobiol.* **1998**, 8, 418-424.

(19) Schumacher, M. A. *Pain Pract.* **2010**, 10, 185-200.

(20) Jalali-Yazdi, F.; Chowdhury, S.; Yoshioka, C.; Gouaux, E. *Cell* **2018**, 175, 1520-1532.

(21) Paoletti, P.; Ascher, P.; Neyton, J. *J. Neurosci.* **1997**, 17, 5711-5725.

(22) Traynelis, S. F.; Hartley, M.; Heinemann, S. F. *Science* **1995**, 268, 873-876.

(23) Chen, B.; Liu, J.; Yang, T.; Chen, L.; Hou, J.; Feng, C.; Huang, C. Z. *Talanta* **2019**, 191, 357-363.

(24) Liu, Y.; Fares, M.; Dunham, N. P.; Gao, Z.; Miao, K.; Jiang, X.; Bollinger, S. S.; Boal, A. K.; Zhang, X. *Angew. Chem. Int. Ed.* **2017**, 56, 8672-8676.

(25) Ning, J.; Wang, W.; Ge, G.; Chu, P.; Long, F.; Yang, Y.; Peng, Y.; Feng, L.; Ma, X.; James, T. D. *Angew. Chem. Int. Ed.* **2019**, 58, 9959-9963.

(26) Khan, M.; Goldsmith, C. R.; Huang, Z.; Georgiou, J.; Luyben, T. T.; Roder, J. C.; Lippard, S. J.; Okamoto, K. *Natl. Acad. Sci. U. S. A.* **2014**, 111, 6786-6791.

(27) Zhu, H.; Fan, J.; Zhang, S.; Cao, J.; Song, K.; Ge, D.; Dong, H.; Wang, J.; Peng, X. *Biomater. Sci.* **2014**, 2, 89-97.

(28) Tang, B.; Yu, F.; Li, P.; Tong, L.; Duan, X.; Xie, T.; Wang, X. *J. Am. Chem. Soc.* **2009**, 131, 3016-3023.

(29) Lee, D.; Swamy, K. M. K.; Hong, J.; Lee, S.; Yoon, J. *Sens. Actuators, B* **2018**, 266, 416-421.

(30) Yamada, T.; Fujiwara, S.; Fujita, K.; Tsuchido, Y.; Hashimoto, T.; Hayashita, T. *Molecules* **2018**, 23, 635-646.

(31) Chen, T.; Pei, X.; Yue, Y.; Huo, F.; Yin, C. *Spectrochim. Acta, Part A* **2019**, 209, 223-227.

(32) Wu, L.; Li, X.; Ling, Y.; Huang, C.; Jia, N. *ACS Appl. Mater. Interfaces* **2017**, 9, 28222–28232.

(33) Han, J.; Burgess, K. *Chem. Rev.* **2010**, 110, 2709–2728.

(34) Lee, L. G.; Berry, G. M.; Chen, C. H. *Cytometry* **1989**, 10, 151-164.

(35) Xu, Z.; Yoon, J.; Spring, D. R. *Chem. Soc. Rev.* **2010**, 39, 1996-2006.

(36) Zhang, W.; Wang, X.; Li, P.; Xiao, H.; Zhang, W.; Wang, H.; Tang, B. *Anal. Chem.* **2017**, 89, 6840-6845.

(37) Coyle, J. T.; Puttfarcken, P. *Science* **1993**, 262, 689-695.

(38) Murphy, T. H.; Miyamoto, M.; Sastre, A.; Schnaar, R. L.; Coyle, J. T. *Neuron* **1989**, 2, 1547–1558.

(39) Lee, H. Y.; Weon, J. B.; Ryu, G.; Yang, W. S.; Kim, N. Y.; Kim, M. K.; Ma, C. J.; *BMC Complementary Altern. Med.* **2017**, 17, 207–213.

(40) Lagadic-Gossmann, D.; Huc, L.; Lecureur, V. *Cell Death Differ.* **2004**, 11, 953-961.

(41) Mulkey, D. K.; Henderson, R. A.; Ritucci, N. A.; Putnam, R. W.; Dean, J. B. *Am. J. Physiol. Cell Physio.* **2004**, 286, C940-C951.

(42) Niu, J.; Fan, J.; Wang, X.; Xiao, Y.; Xie, X.; Jiao, X.; Sung, C.; Tang, B. *Anal. Chem.* **2017**, 89, 7210-7215.

(43) Moda-Sava, R. N.; Murdock, M. H.; Parekh, P. K.; Fetcho, R. N.; Huang, B. S.; Huynh, T. N.; Witztum, J.; Shaver, D. C.; Rosenthal, D. L.; Alway, E. J.; Lopez, K.; Meng, Y.; Nellissen, L.; Grosenick, L.; Milner, T. A.; Deisseroth, K.; Bito, H.; Kasai, H.; Liston, C. *Science* **2019**, 364, 147-158.

(44) Gourley, S. L.; Wu, F. J.; Kiraly, D. D.; Ploski, G. E.; Kedves, A. T.; Duman, R. S.; Taylor. J. R. *Biol. Psychiatry* **2008**, 63, 353-359.

(45) Blendy, J. A. *Biol. Psychiatry* **2006**, 59, 1144–1150.

(46) Bodnoff, S. R.; Humphreys, A. G.; Lehman, J. C.; Diamond, D. M.; Rose, G. M.; Meaney, M. J. *J. Neurosci.* **1995**, 15, 61-69.

(47) David, D. J.; Samuels, B. A.; Rainer, Q.; Wang, J. W.; Marsteller, D.; Mendez, I.; Drew, M.; Craig, D. A.; Leonardo, E. D.; Hen, R. *Neuron* **2009**, 62, 479–493.

(48) Lu, X. Y.; Kim, C. S.; Frazer, A.; Zhang, W. *Proc. Natl. Acad. Sci. U. S. A.* **2006**, 103, 1593-1598.

(49) Petit-Demouliere, B.; Chenu, F.; Bourin, M. *Psychopharmacology* **2005**, 177, 245-255.

(50) Maes, M.; D'Haese, P. C.; Scharpe, S.; D'Hondt, P.; Cosyns, P.; De Broe, M. E. *J. Affective Disord.* **1994**, 31, 135-140.

(51) Hamakawa, H.; Murashita, J.; Yamada, N.; Inubushi, T.; Kato, N.; Kato, T. *Psychiatry Clin. Neurosci.* **2004**, 58, 82-88.

(52) Love, S. *Brain Pathol.* **1999**, 9, 119–131.

(53) Beal, M. F. *Ann. Neurol.* **1995**, 38, 357-366.

(54). Lee S. J.; Koh, J. Y. *Mol. Brain* **2010**, 3, 30–38.

(55). Ruttkay-Nedecky, B.; Nejdl, L.; Gumulec, J.; Zitka, O.; Masarik, M.; Eckschlager, T.; Stiborova, M.; Adam, V.; Kizek, R.; *Int. J. Mol. Sci.* **2013**, 14, 6044-6066.

(56) Betzen, C.; White, R.; Zehendner, C. M.; Pietrowski, E.; Bender, B.; Luhmann, H. J.; Kuhlmann, C. R. W. *Free Radical Biol. Med.* **2009**, 47, 1212-1220.

(57) Wong, E. H.; Kemp, J. A.; Priestley, T.; Knight, A. R.; Woodruff, G. N.; Iversen, L. L. *Proc. Natl. Acad. Sci. U. S. A.* **1986**, 83, 7104-7108.

For TOC